Asian Journal of Pharmaceutical Sciences 13 (2018) 360–372

Available online at www.sciencedirect.com

ScienceDirect

journal homepage: www.elsevier.com/locate/AJPS

Original Research Paper

Intracellular distribution and internalization pathways of guanidinylated bioresponsive poly(amido amine)s in gene delivery☆

Jinmin Zhang[a], *Chunxi Wang*[a], *Mei Lu*[a], *Haonan Xing*[a], *Tianzhi Yang*[b], *Cuifang Cai*[a], *Xiaoyun Zhao*[c], *Minjie Wei*[d], *Jiankun Yu*[e,*], *Pingtian Ding*[a,**]

[a] *School of Pharmacy, Shenyang Pharmaceutical University, Shenyang, 110016, China*
[b] *Department of Basic Pharmaceutical Sciences, School of Pharmacy, Husson University, Bangor, ME, 04401, USA*
[c] *Department of Microbiology and Cell Biology, School of life Science and Biopharmaceutics, Shenyang Pharmaceutical University, Shenyang, 110016, China*
[d] *Department of Pharmacology, School of Pharmacy, China Medical University, Shenyang, 110122, China*
[e] *Department of Ion Channel Pharmacology, School of Pharmacy, China Medical University, Shenyang, 110122, China*

ARTICLE INFO

Article history:
Received 6 August 2017
Revised 26 November 2017
Accepted 26 February 2018
Available online 12 March 2018

Keywords:
Guanidinylated poly(amido amine)s polymers
Nucleolus localization
Cell cycle status
Internalization pathways

ABSTRACT

Guanidinylated bioresponsive poly(amido amine)s polymers, CAR-CBA and CHL-CBA, were synthesized by Michael-type addition reaction between guanidine hydrochloride (CAR) or chlorhexidine (CHL) and N,N′-cystaminebisacrylamide (CBA). Previous studies have shown that both polymers had high transfection efficiencies as gene delivery carriers. In this study, we investigated the nucleolus localization abilities and cellular internalization pathways of these two polymers in gene delivery. Each polymer condensed plasmid DNA (pDNA) and formed nanoparticle complexes, and then their transfection studies were performed in MCF-7 cells. Both complexes were found enriched in nucleolus after cellular transfection, and their transfection efficiencies were significantly improved when transfection was performed on MCF-7 cells arrested at M phase. The transfection efficiency of CAR-CBA-pDNA was inhibited by chlorpromazine, and cell endosomes were disrupted after being exposed to CAR-CBA-pDNA. In regards to CHL-CBA-pDNA, its transfection efficiency was not affected

Abbreviations: AFM, atomic force microscopy; CAR, guanidine hydrochloride; CBA, N,N'-cystaminebisacrylamide; CHL, chlorhexidine; CPPs, cell- penetrating peptides; DAPI, 2-(4-Amidinophenyl)-6-indolecarbamidine dihydrochloride; DiI, 1,1′-dioctadecyl-3,3,3′,3′-tetramethylindocarbocyanine perchlorate; DLS, dynamic light scattering; DMEM, Dulbecco's Modification of Eagle's medium; PAAs, poly(amido, amine)s; EGFP, enhanced green fluorescent protein; Gua-SS-PAAs, guanidinylated disulfide containing poly(amido amine) polymers; LDH, Lactate dehydrogenase; NMR, nuclear magnetic resonance; NOR, nucleolar organizing region; OD, optical density; pDNA, plasmid DNA; rRNA, ribosomal RNA; SS-PAAs, disulfide containing poly(amido, amine).

☆ Peer review under responsibility of Shenyang Pharmaceutical University.

* Corresponding author at: Department of Ion Channel Pharmacology, School of Pharmacy, China Medical University, Shenyang, 110122, China. Tel.: 86-24-23986305

** Corresponding author: Shenyang Pharmaceutical University, No. 85, Economic and Technological Development Zone, Benxi 117004, China. Tel.: 024-43520515

E-mail addresses: 267204521@qq.com (J. Yu), dingpingtian@qq.com (P. Ding).

https://doi.org/10.1016/j.ajps.2018.02.008

by three types of endocytosis inhibitors used in the study, and CHL-CBA-pDNA showed no effect on endosomes. Cellular lactate dehydrogenase release and membrane morphology were changed after cells were transfected by the two complexes. The results indicated that both CAR-CBA and CHL-CBA polymers demonstrated good nucleolus localization abilities. It was beneficial for transfection when cells were arrested at M phase. CAR-CBA-pDNA cellular internalization was involved with clathrin-mediated endocytosis pathway, and escaping from endosomal entrapment, while the cellular uptake of CHL-CBA-pDNA occurs via clathrin- and caveolae-independent mechanism.

1. Introduction

Gene therapy has been widely used to deliver functional genetic materials into cells to compensate for the malfunctioning genes or to make beneficial proteins. Viral and nonviral gene carriers are two main families in delivering exogenous genetic materials to host cells. There are many advantages of viral vectors, such as high transfection efficiency and long term gene expression by integrating genes into host cells' genome [1]. However, the potential immunogenicity and oncogenic effects are the biggest safety issues that limit viral vectors' applications in gene therapy [2,3]. Thus, nonviral gene carriers, especially cationic polymers, have become more preferred alternatives due to their better safety characteristics after administration [4]. Cationic polymers, poly(amido, amine)s dendrimers (PAAs) [5], have been reported to possess many other characteristics, such as better storage stability, low immunogenic response, satisfactory DNA loading capacity, and convenience in manufacturing and handling [6]. SS-PAAs, which are water-soluble, peptidomimetic polymers, could be obtained by Michael-type polyaddition reaction between cystamine bisacrylamide and primary or bis-secondary amine monomers [7]. This reaction could produce a number of SS-PAAs with various functional groups in polymeric main or side chain. For example, SS-PAAs could rapidly disintegrate into low molecular weight fragments after uptake into the target cells [8].

The nuclear envelop is the main obstacle for non-viral gene carriers to deliver exogenous genes into nucleus, and even nucleolus. Nuclear envelop, having two phospholipid bilayers, isolates nucleus from cytoplasm. Nucleolar organizing region (NOR), a part of nucleolus, plays an important role in nucleolus reassembly and gene expression. Moreover, ribosomal RNA (rRNA) transcription and ribosome biogenesis proceed in nucleolus [9]. Researchers reported that proteins of viral vectors, such as HIV-1 TAT could target the host cells' nucleolus and assist viral genome to replicate and transcribe [10]. Two approaches have been applied to overcome the obstacle of nuclear envelop. The first one is by making use of cell proliferation process. The nuclear envelope breaks down in mitosis (M phase), which gives the exogenous DNA more chances to get into nucleus [11,12]. The second approach is by introducing nuclear envelop penetration and nuclear targeting factors mimicking viral vectors' protein. For example, cell penetrating peptides (CPPs) have transmembrane ability [13], and HIV TAT peptide, a kind of CPPs, has not only cell and nuclear transmembrane ability but also nucleolus targeting ability [10,14]. It has been reported that liposomes-pDNA complexes modified with TAT peptide, showed improved transfection *in vitro* and *in vivo* [15]. However, when cationic polymers noncovalently combined with these proteins or peptides, their abilities of DNA condensation were reduced, and the complexes became more complicated and unstable. Therefore, amine monomers with multifunctional groups need to be introduced to cationic polymers, giving these polymers membrane penetration, and nucleolus localization abilities without being trapped in endosomes. For example, as guanidino groups are functional groups in CPPs [16], a hypothesis was proposed that guanidino group could delocalize the charges present on primary amines of polymers [17], and further help reduce cytotoxicity of cationic polymers.

A bilayer of lipids and incorporated proteins comprise cell membrane, which defines the cell by isolating the intracellular substance from the extracellular environment. Cell membrane mediate the interchange of materials between extracellularsetting and intracellular matrix via active or passive transport [18]. Macromolecule internalization occurs mostly through receptor-mediated endocytosis, such as clathrin-mediated, caveolae-mediated, macropinocytosis and clathrin- and caveolae-independent endocytosis [19], and the uptake mechanisms of exogenous materials are determined by their physicochemical properties, such as size, surface functionalization, geometry [20,21]. Moreover, the endocytosis mechanisms are linked with the intracellular transport and the fate of the exogenous materials [22]. For example, clathrin-mediated endocytosis was reported to correlate with the acidic lysosomes [23,24], and PEI was an excellent case to demonstrate the endosomal/lysosomal escape with a hypothesis of "proton sponge effect" [25]. While, internalization via caveolae-mediated and macropinocytosis endocytosis are neither acidic nor digestive, therefore, this could avoid lysosomal degradation in these process [26]. Some types of liposomes/lipids were reported to deliver gene by caveolae-mediated endocytosis [27].

Guanidine groups play an important role in CPPs [16], such as HIV TAT peptide [13], and Kim et al. have reported that guanidinylated bioreducible polymer have high nuclear localization ability as gene carriers [28]. Polymers of CAR-CBA and CHL-CBA, which belong to guanidinylated disulfide containing poly(amido amine) polymers (Gua-SS-PAAs), are synthesized

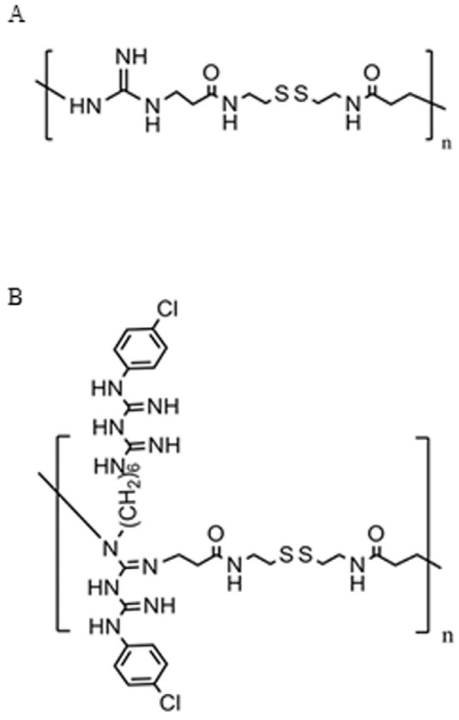

Fig. 1 – Chemical structures of guanidinylated polymers (A) CAR-CBA and (B) CHL-CBA [29].

by Yu et al. based on the mechanism of Michael-addition polymerization. There are disulfide bonds and guanidino groups in the two polymers (Fig. 1) [29]. The disulfide bonds make the two polymers disintegrate into low molecular weight fragments in the intracellular environment, which decreases the cytotoxicity and affinity between DNA and polymers, and the guanidinylated polymers are designed as "virus like vectors" mimicking the HIV TAT peptide. All these characteristics make guanidinylated polymers as potential excellent gene delivery carriers [29]. However, no study has been reported how these polymers mediate the cellular gene transfection pathways. In this study, we explored the *in vitro* nucleolus localization ability and transfection mechanisms of these two Gua-SS-PAAs polymers, CAR-CBA and CHL-CBA, as gene delivery carriers.

2. Materials and methods

2.1. Materials

Thymidine, Chlorpromazine, Colchicine and indomethacin were purchased from Solarbio (Beijing, China). Hochest33342, 2-(4-Amidinophenyl)-6-indolecarbamidine dihydrochloride (DAPI), 1,1′-dioctadecyl-3,3,3′,3′-tetramethylindocarbocyanine perchlorate (Dil) and Lactate dehydrogenase (LDH) Release Assay Kit were purchased from Beyotime Biotechnology (Jiangsu, China). Lyso-ID Red Lysosomal Detection Kit and Nucleolar-ID Green Detection Kit (GFP-Certified) were purchased from ENZO Life Science (Missouri, USA). Cell Cycle Detection Kit was purchased from Keygen Biotech (Nanjing, China). TIANpure Midi Plasmid Kit was purchased from Tiangen Biotech (Beijing, China). MCF-7cells and *Escherichia coli* containing pcDNA3.1-EGFP were provided as gifts from the Department of Pharmacology Teaching and Research Department at China Medical University. CBA was purchased from Alfa Aesar (MA, USA). 2, 2, 4, 6, 7-Pentamethydihydrobenzofuran-5-sulfonyl chloride (Pbf-Cl), CAR, and CHL were purchased from Sinopharm Chemical Regent (Shanghai, China).

2.2. Synthesis of CAR-CBA and CHL-CBA

The synthesis of the two polymers were reported by Yu et al. [29]. Briefly, there were three main reactions. In the first reaction, Pbf-Cl was used to activate the guanidine group. CAR or CHL acetate was dissolved in water, and Pbf-Cl was dissolved in acetone. Then the Pbf-Cl solution was added to the CAR or CHL solution dropwise at a temperature range of 0 °C to 3 °C, and the mixture was stirred for 3 h at room temperature. In this reaction, the 4 M NaOH solution was used to maintain the systemic pH at 11–12. At the end point of the first reaction, the white resultants precipitate (CAR-Pbf-Cl or CHL-Pbf-Cl) was collected via filtration. The second reaction was Michael addition polymerization between CBA and CAR/CHL at 60 °C in a dark and nitrogen atmosphere for approximate one week. After that 10% excess of CAR/CHL-Pbf-Cl was added and the reaction was kept for another 2 d. The third reaction was the de-protection of Pbf-Cl. Trifluoroacetic acid, triisopropylsilane and water under a certain ratio were added to the resultant of the second reaction. The mixture was stirred at room temperature for 3 h. Then the resultant was collected and dialyzed for 2 d. At last, the solution was lyophilized. The molecular weight of CAR-CBA and CHL-CBA are around 10,595 Da and 7609 Da, respectively [29,30].

2.3. Plasmid purification of pcDNA3.1-EGFP

pcDNA3.1-EGFP plasmids, which encode enhanced green fluorescent protein (EGFP) and ampicillin resistance gene, were transformed into *E. coli*, and the transformed bacteria inoculated into Luria-Bertanic culture media containing 100 μg/ml ampicillin, and then shaken overnight at 37 °C, and 200 r/min. The pDNA was purified from the transformed bacteria using TIANpure Midi Plasmid Kit in accordance with the manufacturer's instructions. The concentration of purified pDNA was determined by measuring its ultraviolet absorbance at 260 nm using Nanodrop 2000 (Thermo Scientific, Waltham, MA). The purified pDNA was used for further experiments when its optical density (OD) ratio of OD_{260}/ OD_{280} was in the range of 1.8 to 2.0.

2.4. Cell culture

MCF-7 cells, a type of human breast cancer cells, were cultured in full Dulbecco's Modification of Eagle's medium (DMEM) at 37 °C with a humidified 5% CO_2/95% air containing atmosphere. The full medium was made by adding 10% (v/v) fetal bovine serum, 100 U/ml penicillin G sodium, and 100 μg/ml streptomycin sulfate into serum free medium.

2.5. Preparation of DAPI labeled pDNA

Firstly, 1 μl DAPI (5 mg/ml) and 2 μg of pDNA solution (400 ng/μl) were mixed by vortex for 10 sec, and incubated at 37 °C for 1 h. Secondly, the DAPI labeled pDNA was precipitated with 70% ethanol and centrifuged at 12 000 r/min for 10 min. Finally, the precipitation was re-suspended in Tris Buffer. The DAPI labeled pDNA was freshly prepared each time before being used for further experiments.

2.6. Complex preparation and characterization

To prepare complexes of CAR-CBA-pDNA and CHL-CBA-pDNA at polymer/pDNA weight ratio (w/w) of 24/1, 48 μg of CAR-CBA and 48 μg of CHL-CBA were dissolved in each 500 μl serum free medium. Afterwards, each polymer solution was added to 2 μg of pDNA in 500 μl serum free medium. The polymer-pDNA solutions were then vortexed for 10 sec, and incubated for 10 min at room temperature to form complexes. Complexes were prepared freshly prior to each transfection study.

A Zetasizer Nano system equipped with dynamic light scattering (DLS) was used to measure the particle size, size distribution and zeta potential. Meanwhile, the morphology of complex was investigated using atomic force microscopy (AFM) [29]. The zeta potentials of complexes are around + 30 mV (CAR-CBA-pDNA) and + 15 mV (CHL-CBA-pDNA). Most pDNAs could be condensed into nano-scaled particles (less than 50 nm) by these polymers.

2.7. Nucleolus localization of complexes

Naked DAPI-labeled pDNA and DAPI-labeled complexes (CAR-CBA-pDNA and CHL-CBA-pDNA), in which the pDNA was labeled with DAPI, were prepared as the sections of 2.5 and 2.6. MCF-7 cells were seeded into 6-well plates containing coverslips in each well. Transfection was operated when cells reached 60% confluency. Cells were exposed to CAR-CBA-pDNA, CHL-CBA-pDNA, and naked DAPI labeled pDNA (served as a negative control), respectively, for 4 h. At the end of transfection, the transfected cells were washed with phosphatebuffered saline (PBS), and then stained with Nucleolar-ID Green Detection Kit at 37 °C for 15 min in accordance with the protocol provided by the manufacturer. The cells were then washed with PBS, and finally fixed in 4% formaldehyde for 15 min. The transfected cells of each treatment group were observed and their images were recorded immediately with the ECLIPSE 80i fluorescence microscope (Nikon, Tokyo, Japan) equipped with 40 × objective lens. The intracellular exogenous substances and intracellular nucleolus appeared to be in blue and green colors, respectively.

2.8. Cell synchronization and cell cycle status analysis

Double- thymidine block and colchicine were used to induce and arrest cells at specific cell cycle phases. In double-thymidine block, cells could be arrested at G1, S, or G2 phases during the second release, and the time period of each block and release stage changes with different cell lines [31]. As for the treatment of colchicine, cells could be arrested at M phase. In this study, MCF-7 cells were seeded into 6-well plates. For double-thymidine block treatment, cells were treated with 2 mM thymidine in full medium for 16 h (first block) when cells reached around 30% confluency. Afterwards, the medium with thymidine was discarded, and the cells were washed with PBS, and then fresh full medium without thymidine was added to the cell plates. After that the cells were cultured for another 10 h (first release). At the end of first release, the medium was replaced with fresh full medium with 2 mM thymidine for another 16 h incubation (second block). At last, the cells were washed with PBS and released in thymidine-free medium for 0 h, 4 h or 8 h (second release), and then the cells at each end time point of second release were collected. For the colchicine treatment, cells with 60% confluency, were exposed to 0.4 μg/ml of colchicine (final concentration) in full medium for 16 h, and the cells were collected for further analysis. Un-induced cells were collected as a negative control when they arrived at 60% confluency.

The collected cells by various treatments were fixed in 70% cold ethanol at 4 °C for overnight. To analyze DNA content of the cells, Cell Cycle Detection Kit was used, and the detailed procedures were performed in accordance with the manufacturer's protocols. Subsequently, the DNA content of collected cells (stained with PI) in each group was analyzed by the FACSCalibur flow cytometer (BD, New Jersey, USA) equipped with Modfit LT3.0 software, and 10 000 cells were analyzed in each treatment group.

The DNA content analysis cannot be used solely to differentiate between cellular G2 and M phases, while the nuclear morphological characteristics of the two phases are distinctly different, Therefore, DNA content coupled with nuclear morphology could help us ascertain if the cells were arrested at G2 and M phases as expected. In order to observe the nuclear morphologies of cells after thymidine or colchicine treatment, cells were seeded into 6-well plates with coverslips, and then went through 8 h of thymidine second release treatment or exposed to colchicine in full medium for 16 h, then the cells were stained with 10 μg/ml of Hochest33342 at room temperature for 10 min. After being washed with PBS, the nuclear morphologies of Hochest33342 stained cells were observed and recorded immediately by the ECLIPSE 80i fluorescent microscope (Nikon, Tokyo, Japan) equipped with 40 × objective lens.

2.9. Transfection on cells arrested at various cell cycle phases

Transfection was performed on MCF-7 cells arrested at various cell cycle phases (G1, S, G2, and M phase) or un-induced cells. Cells of each group were exposed to CAR-CBA-pDNA, CHL-CBA-pDNA and naked pDNA, respectively, in serum free medium for 4 h, then the complexes and naked pDNA containing medium was discarded. Subsequently, the cells were washed with PBS, and incubated in full medium for another 48 h. At the predetermined time point, EGFP intensity of the transfected cells in each group was recorded by the LSR-Fortessa flow cytometer (BD, New Jersey, USA) equipped with FACADiva 7.0 software, and 10 000 cells were analyzed in each treatment group. Cells exposed to the naked pDNA were set as a negative control.

2.10. *Transfection on cells with treatment of endocytosis inhibitors*

According to previous reports, chlorpromazine, colchicine, and indomethacin were used as endocytosis inhibitors to inhibit clathrin-mediated, macropinocytosis and caveolae-mediated endocytosis, respectively [32–34]. In this study, MCF-7 cells were seeded into 6-well plates. When the cells reached 60% confluency, they were cultured in serum free medium for 30 min. Subsequently the medium was replaced with serum free medium containing 10 μg/ml of chlorpromazine, 8 μg/ml of colchicine, or 6 μg/ml of indomethacin, or drug free medium, and the cells were incubated for another 1 h. Each group of pretreated cells were then exposed to serum free medium containing CAR-CBA-pDNA or CHL-CBA-pDNA, respectively, for 4 h, while the concentrations of endocytosis inhibitors were kept the same as pretreatments in each group. At the end of transfection, all treatment solutions were discarded. After being washed with PBS, the cells in each group were cultured in fresh full medium for an additional 48 h. EGFP intensity of transfected cells in each group was recorded by the LSRFortessa flow cytometer (BD, New Jersey, USA) equipped with FACADiva 7.0 software, and 10 000 cells were analyzed for each treatment group. The group of cells exposed to the naked pDNA for 4 h in serum free medium was set as a negative control.

2.11. *Endosomal escape of complexes*

DAPI was used to label naked pDNA or pDNA in the complexes of CAR-CBA-pDNA and CHL-CBA-pDNA as the sections of 2.5 and 2.6. MCF-7 cells were seeded into glass-bottom cell culture dishes and cultured in full medium at 37 °C in a humidified 5% CO_2/95% air containing atmosphere. After reaching 60% confluency, the cells were washed with PBS and exposed to DAPI-labeled complexes (CAR-CBA-pDNA and CHL-CBA-pDNA), naked DAPI-labeled pDNA (served as a negative control), or chloroquine (300 μM final concentration, served as a positive control), respectively, in serum free medium for 4 h. At the end of transfection, the DAPI-labeled complexes, naked DAPI-labeled pDNA, and chloroquine containing solutions were discarded. Then the cells in each group were washed with PBS, and stained with Nucleolar-ID Green Detection Kit for 15 min, then washed with PBS. After that the cells were stained with Lyso-ID Red Lysosomal Detection Kit for 15 min. The staining procedures were performed in accordance with the protocols provided by manufactures. After being washed with PBS, The stained cells in each group were fixed in 4% formaldehyde for 15 min, and then the stained cells were observed and their images were captured immediately by the FV1000S-SIM/IX81 confocal laser scanning microscopy (OLYMPUS, Tokyo, Japan) equipped with 60 × oil immersion objective lens. The intracellular nucleolus, endosomes/lysosomes, and DAPI labeled exogenous substances appeared to be in green, red and blue colors, respectively.

2.12. *Lactate dehydrogenase release assay*

MCF-7 cells were seeded into 96-well plate at a density of 5000 cells/well, and incubated in full medium at 37 °C in a hu-

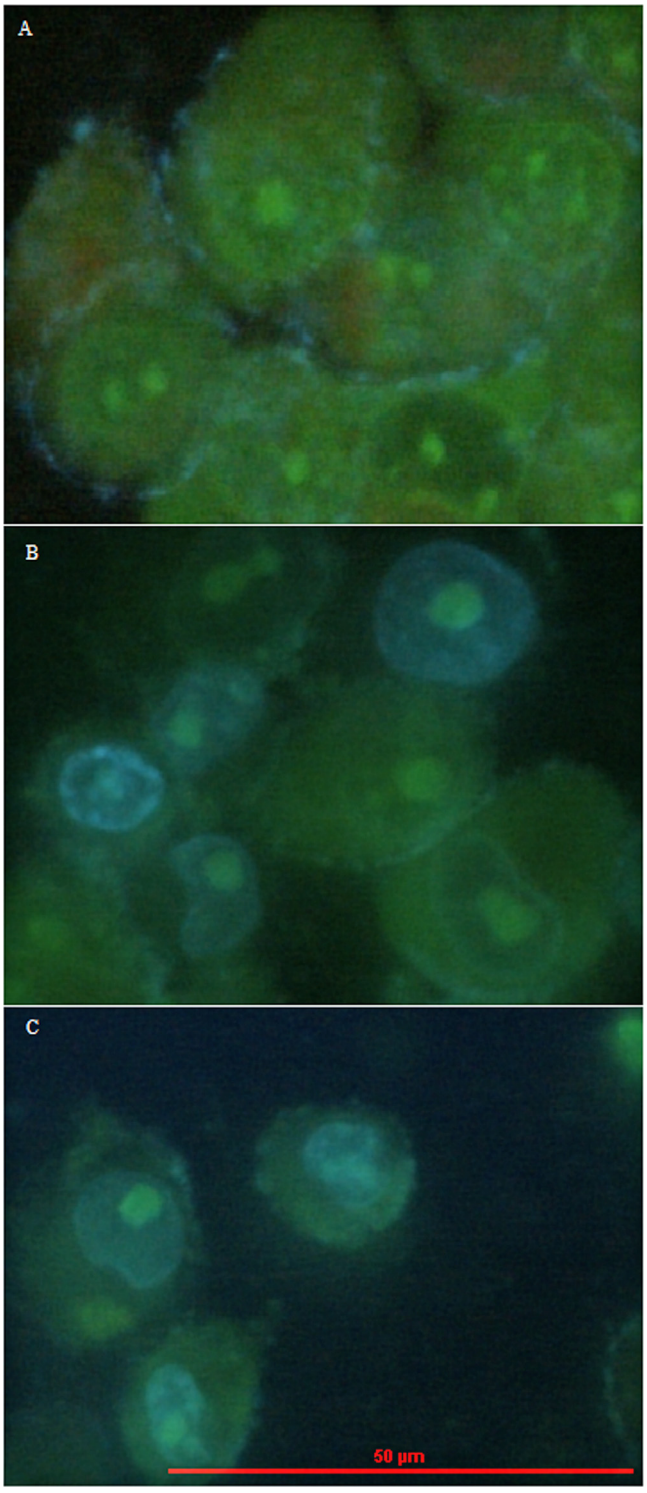

Fig. 2 – Nucleolus localization of the: (A) naked DAPI-labeled pDNA (negative control), (B) CAR-CBA-pDNA, and (C) CHL-CBA-pDNA recorded by fluorescence microscopy, where the DAPI-labeled exogenous substances were shown in blue color, nucleolus was shown in green color, and the scale bar corresponds to 50 μm.

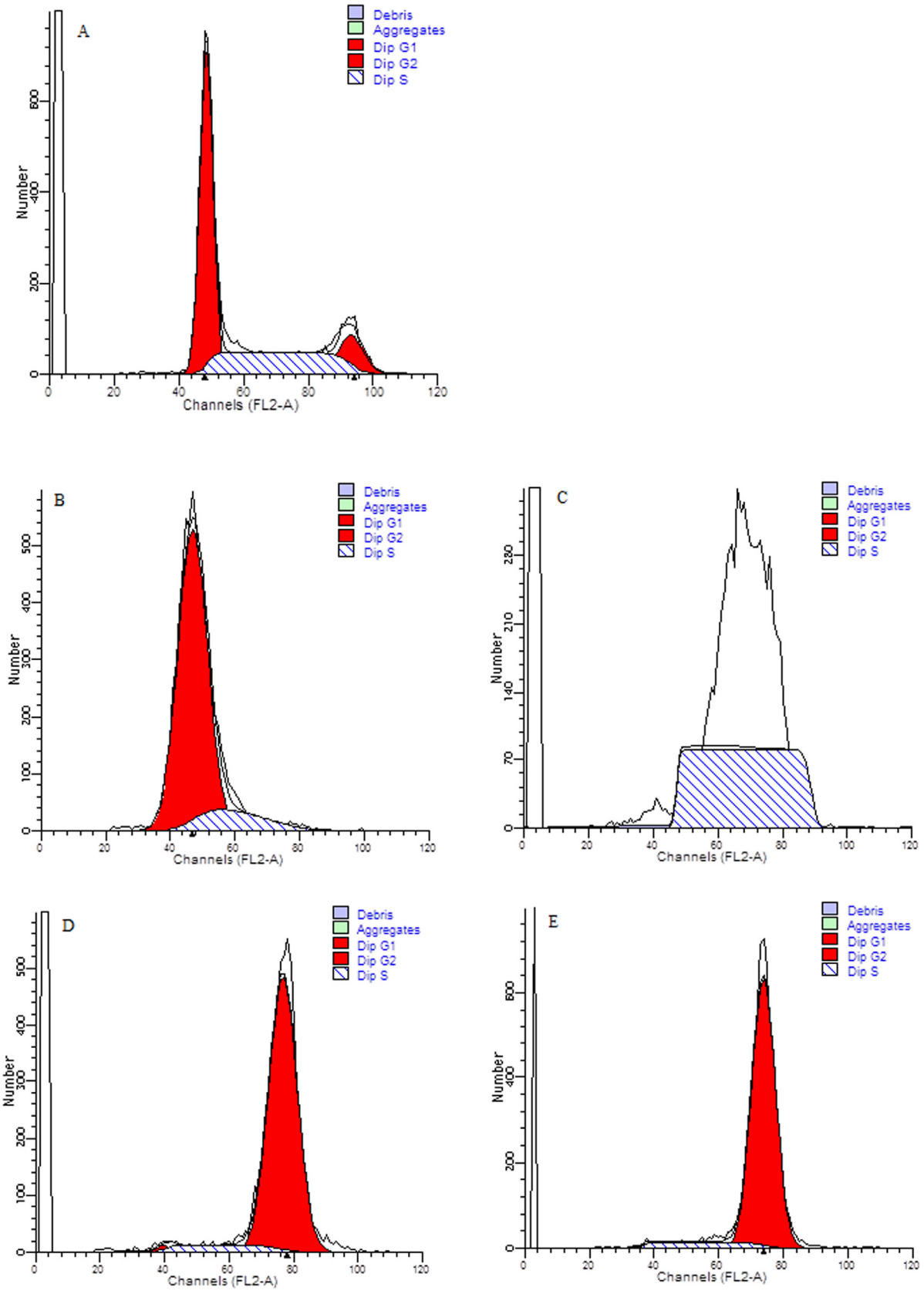

Fig. 3 – DNA content of MCF-7 cells under different synchronization treatments of: (A) uninduced, (B) 0 h release, (C) 4 h release, (D) 8 h release, and (E) colchicine, analyzed by flow cytometry with PI staining.

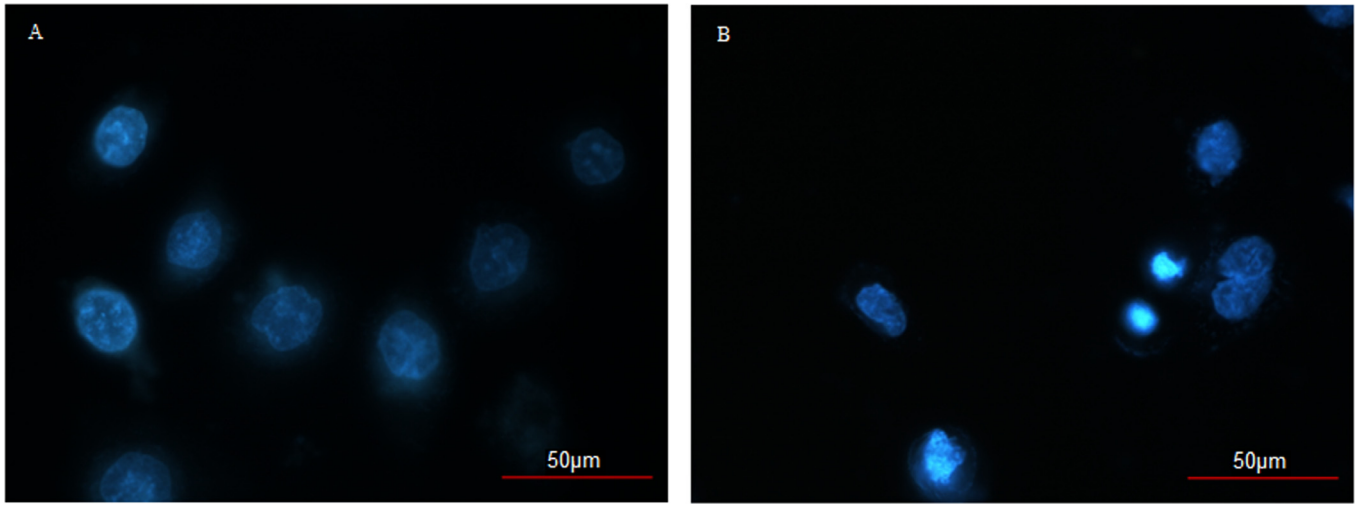

Fig. 4 – Nuclear morphological images of cells stained by Hoechst 33,342 at the end time point of: (A) 8 h release in double-thymidine block, and (B) 16 h in colchicine treatment. The images were recorded by fluorescence microscopy. The scale bar corresponds to 50 μm.

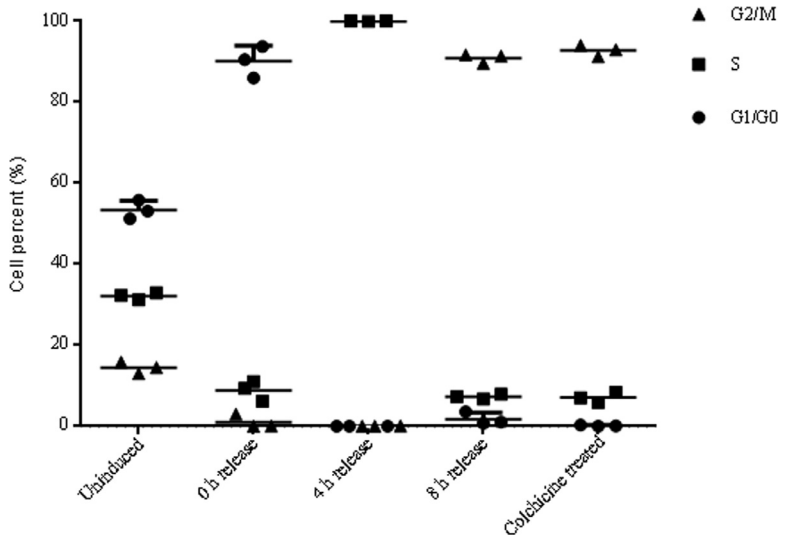

Fig. 5 – Percentages of cells arrested at each cell phase under various synchronization treatments. Data were shown in means ± SD.

midified 5% CO_2/95% air containing atmosphere. When cells reached 60% confluency, they were washed with PBS, and then, respectively, exposed to naked pDNA (served as a negative control), CAR-CBA-pDNA, or CHL-CBA-pDNA in 150 μl serum free medium, or only to 150 μl serum free medium (served as a positive control). At the third h, 15 μl of LDH release reagent was added to the positive control group. After reaching the predetermined time point of 4 h, the quantity of LDH, which was released to the medium supernatant or remained inside of cells in the same well of each treatment group, was measured using a LDH Release Assay Kit in accordance with the protocols. The optical densities were recorded by the iMark microplate reader (Bio-rad, Tokyo, Japan) at 492 nm with 620 nm as a reference wavelength. For each treatment, the LDH release ratio was calculated by the following formula,

where $OD_{release}$ means optical density of LDH in supernatant solution; OD_{cell} means optical density of LDH detained in cells; OD_{blank} means optical density of LDH in blank medium.

$$\text{LDH release}(\%) = \frac{OD_{release} - OD_{blank}}{OD_{cell} - OD_{blank} + OD_{release} - OD_{blank}} \times 100$$

2.13. *Morphology of cell membrane after transfection*

Triton X-100, a detergent, can destabilize cell membrane structure and cause membrane disruption [35]. So Triton X-100 treated cells were served as a positive control to show the morphology changes of cell membrane after being penetrated in this study. MCF-7 cells were seeded into 6-well plates containing coverslip in each well. When cells reached 60% conflu-

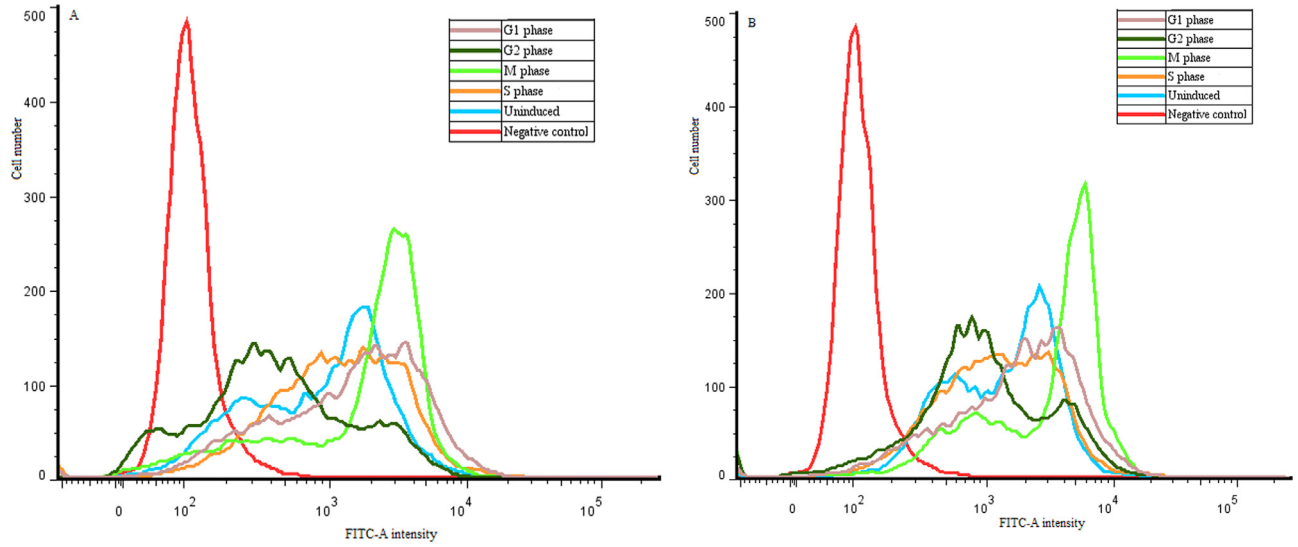

Fig. 6 – EGFP intensity of MCF-7 cells arrested at various cell cycles after the treatments of: (A) CAR-CBA-pDNA and (B) CHL-CBA-pDNA. Data were recorded by flow cytometry, and analyzed by FloJo 7.6.1. Cells treated with naked pDNA were set as a negative control.

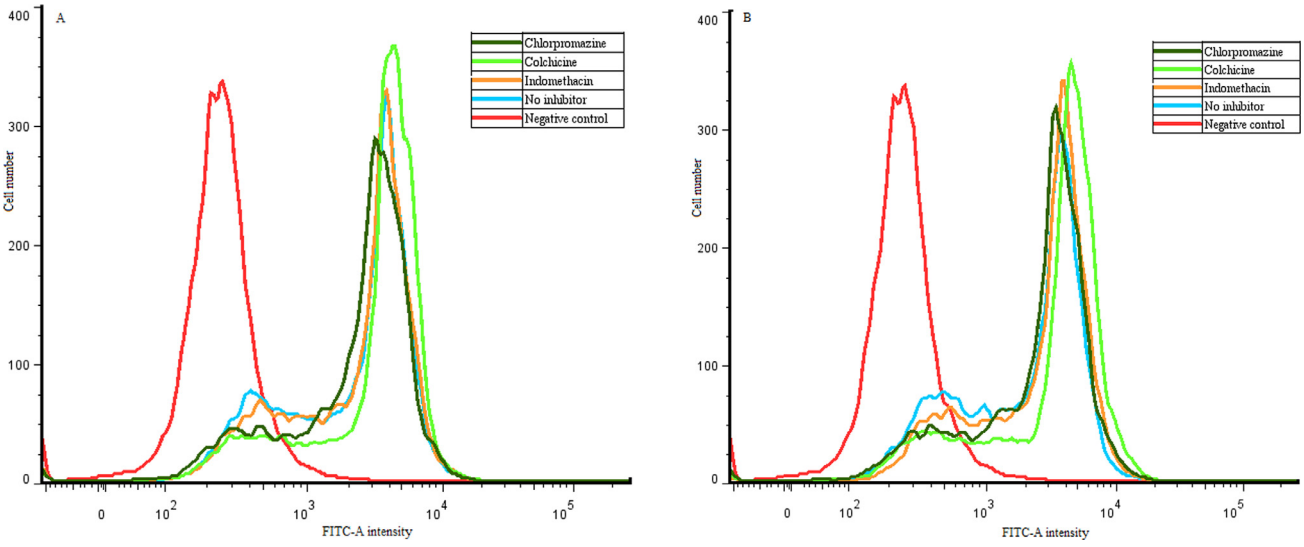

Fig. 7 – EGFP peak intensities of MCF-7 cells transfected by: (A) CAR-CBA-pDNA and (B) CHL-CBA-pDNA) with or without pretreatments of chlorpromazine (10 mg/ml, related to clathrin-mediated endocytosis), colchicine (8 mg/ml, related to macropinocytosis), and indomethacin (6 mg/ml, related to caveolae-mediated endocytosis). Data were recorded by flow cytometry, and analyzed by FloJo 7.6.1. Cells treated with naked pDNA were set as a negative control.

ency, they were exposed to CAR-CBA-pDNA, CHL-CBA-pDNA, naked pDNA (served as a negative control), and 1% Triton-X 100 (served as a positive control), respectively, in serum free medium for 4 h at 37 °C in a humidified 5% CO_2/95% air containing atmosphere. At the end of transfection or treatments, the cell membrane in each group was stained with 8 mM DiI in PBS for 15 min at 37 °C. After being washed with PBS, the cell membranes of transfected cells were observed and their images were recorded immediately by the ECLIPSE 80i fluorescence microscope (Nikon, Tokyo, Japan) equipped with 100 × oil immersion lens. The cell membrane appeared to be in red color.

2.14. *Statistical analysis*

Statistical analyses were performed with a tool of GraphPad Prism, version 6 software (GraphPad Software Inc., California,

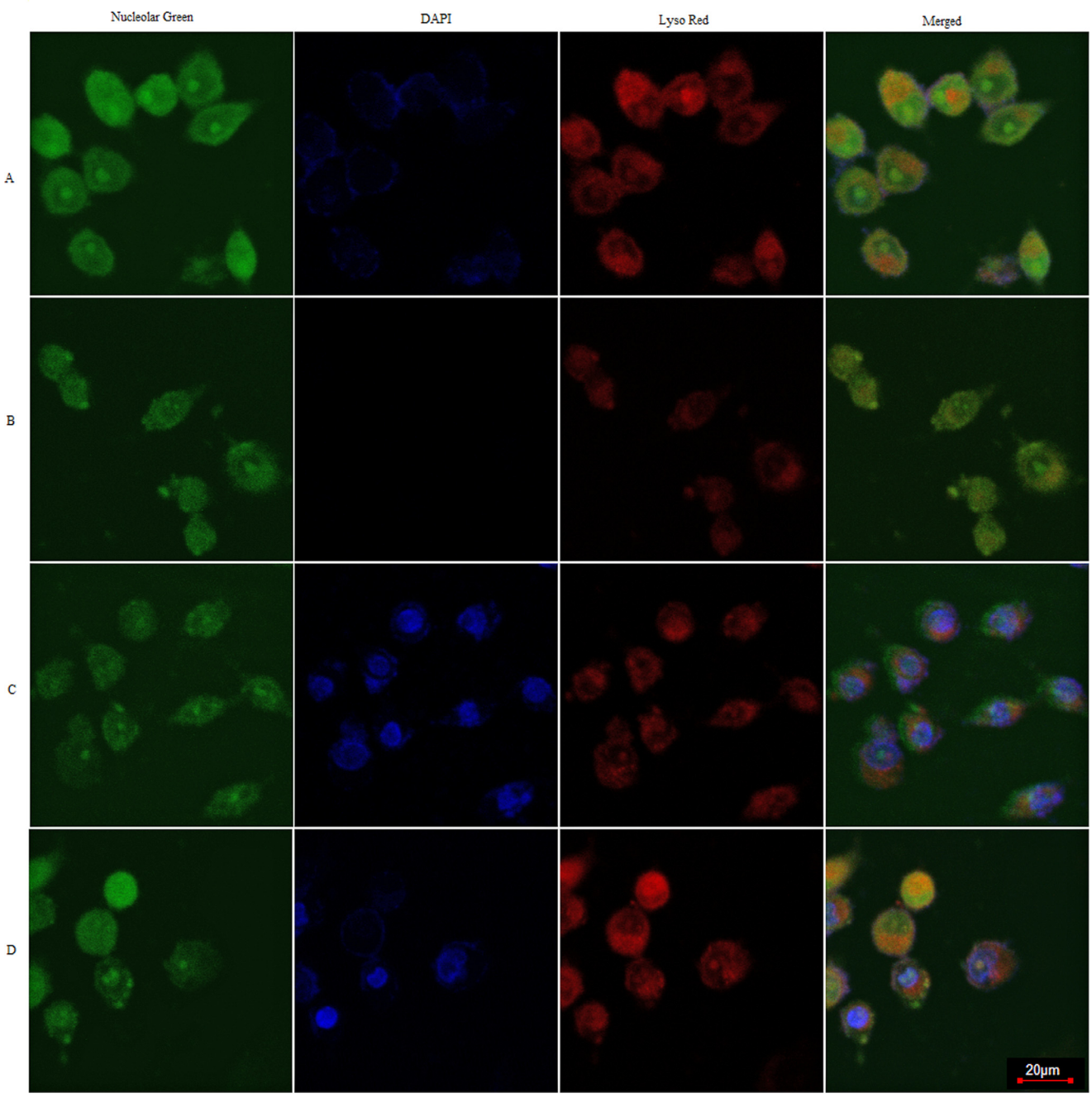

Fig. 8 – Fluorescent intensity reflecting the endosomal escape abilities of: (A) naked pDNA (set as the negative control), (B) chloroquine treatment (set as the positive control), (C) CAR-CBA-pDNA, and (D) CHL-CBA-pDNA. The images were recorded by confocal laser scanning microscopy, where intracellular nucleolus was shown in green color, the DAPI-labeled exogenous substances were shown in blue color, and intracellular acidic compartments (endosomes/lysosomes) were shown in red color. The scale bar corresponds to 20 μm.

USA). The quantitative results were expressed as mean ± SD from triplicate experiments performed in parallel, and the difference was considered statistically significant when a $P < 0.05$ in two-tailed unpaired Student's *t*-test.

3. Results and discussion

3.1. *Nucleolus localization abilities of complexes*

Naked DAPI-labeled pDNA was set as a negative control in this study to show that no false-positive results were caused by

experimental design method. As shown in Fig. 2A, the naked pDNA (in blue color) appeared around cell membrane, and almost no pDNA existed in the nucleolus. While for CAR-CBA-pDNA and CHL-CBA-pDNA, it was obvious that the two complexes were enriched in or around nucleolus region after cellular transfection (Fig. 2B and C), which suggested that the two guanidio-rich polymers had significant nucleolus localization abilities.

3.2. *Transfection efficiencies change with cell cycle status*

As mentioned before, DNA content analysis could not ascertain the cells with double DNA contents were arrested at G2 or M phase. However, chromosome segregation happens in M phase, which does not happen in G2 phase [36]. The results in Fig. 3 coupled with Fig. 4 showed that, at the end time points of 0 h, 4 h, and 8 h release in double thymidine block and after the treatment of colchicine, the percentages of cells arrested at G1, S, G2, and M phases were 90.07% ± 3.90%, 99.98% ± 0.04%, 90.88% ± 1.11%, and 92.74% ± 1.41%, respectively. The phase ratios of un-induced cells at G1/G0, S, and G2/M phase were 53.38% ± 2.28%, 32.16% ± 0.86%, and 14.46% ± 1.43%, respectively (Fig. 5). These results confirmed that double-thymidine block and colchicine treatments could effectively arrested cells at G1, S, G2, and M phase as we expected.

The EGFP intensity peak height and position reflect the tranfection efficiencies. The higher and more rightward of the EGFP peak is, the more transfection efficiency could be reached. As shown in Fig. 6, after these cells were transfected by CAR-CBA-pDNA and CHL-CBA-pDNA, respectively, the EGFP intensity peaks of cells arrested at M phase were higher and more rightward than these of cells at other cell cycles (i.e., un-induced, G1, S, and G2 phase), and the peak position of cells arrested at G2 phase were more leftward than cells at un-induced, G1, and S phase. Therefore, in terms of height and position of EGFP intensity peak, the transfection efficiencies of CAR-CBA-pDNA and CHL-CBA-pDNA on cells arrested at M phase is higher than that on cells at other phases (i.e., un-induced, G1, S, and G2), while the transfection efficiencies on cells arrested at G2 phase are lower than that on cells at un-induced, G1, and S phase. Overall, MCF-7 cells arrested at M phase are in favor of the transfection efficiencies of the two polymers, and it is unadvisable to perform transfection on cells arretd at G2 phase.

3.3. *Transfection efficiencies change with endocytosis inhibitors*

Similarly, the EGFP intensity peak height and position were used to reflect the tranfection efficiencies. As shown in Fig. 7A, the peak height of EGFP intensity of cells transfected by CAR-CBA-pDNA with chlorpromazine pretreatment was lower than cells transfected by CAR-CBA-pDNA without inhibitor pretreatment, and the peak position of the former was more leftward than the latter. While, the EGFP intensity peaks of cells transfected by CHL-CBA-pDNA with these three types of inhibitors pretreatments were neither lower nor more leftward than cells transfected by CHL-CBA-pDNA without inhibitor pretreatment (Fig. 7B). Thus, the transfection efficiency of CAR-CBA-pDNA was decreased under the pretreatment of chlorpromazine, while the transfection efficiency of CHL-CBA-pDNA was not decreased by the pretreatments of these three endocytosis inhibitors.

3.4. *Endosomal escape abilities of complexes*

Chloroquine is a type of lysosomotropic agent, which could accumulate in the endosomes/lysosomes [37]. When chloroquine enters lysosomes, it is protonated in the organelles with low pH, causing its accumulation. Chloroquine accumulation leads to the swell of endosomes/lysosomes, and then destabilization or rupture of endosomal/lysosomal membrane [38]. When the rupture of endosomal/lysosomal membrane happens, the fluorescent intensity of Lyso-Tracter (an endosomal/lysosomal dye) becomes weaker [39]. As shown in Fig. 8, compared to the negative control (treated with naked pDNA), cells treated by CHL-CBA-pDNA demonstrated no significant difference in the red fluorescence intensity in acidic compartments. As for the positive control (treated with 300 μM chloroquine for 4 h), the red fluorescence intensity in acidic compartments became significantly weaker. For the cells treated by CAR-CBA-pDNA, the intensity of red color became slightly weaker compared to the negative control. From the above results, we could conclude that the complex of CAR-CBA-pDNA is entrapped in endosomes/lysosomes, but it has the ability of endosomal/lysosomal escape, while CHL-CBA-pDNA could keep itself away from .endosomal/lysosomal entrapment.

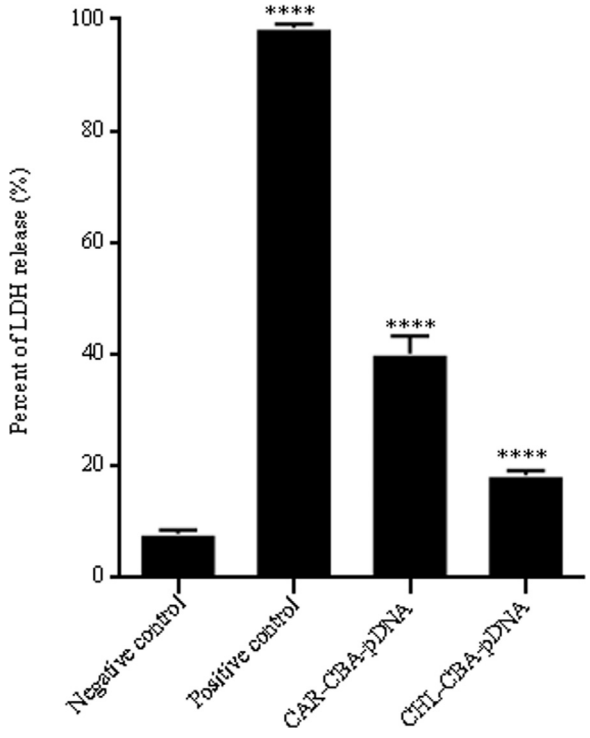

Fig. 9 – LDH release level of MCF-7 cells incubated with naked pDNA (set as a negative control), and LDH release reagent (set as a positive control), CAR-CBA-pDNA, and CHL-CBA-pDNA, respectively. Data were shown in mean ± SD, ** indicates $P < 0.0001$ compared to the negative control.**

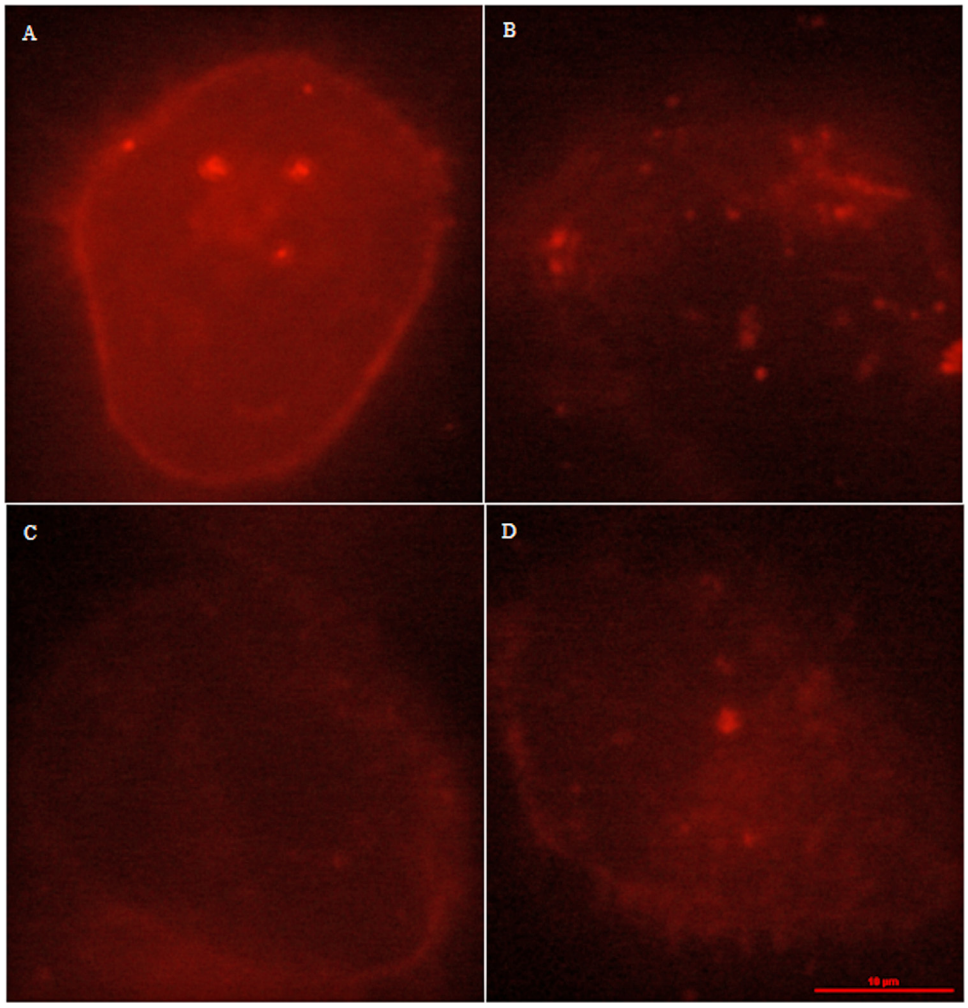

Fig. 10 – Images of cell membrane incubated with: (A) naked pDNA (negative control), (B) 1% Triton X-100 (positive control), (C) CAR-CBA-pDNA, and (D) CHL-CBA-pDNA, respectively. The images were recorded by fluorescence microscopy, and the scale bar corresponds to 10 μm.

3.5. *Lactate dehydrogenase release assay*

LDH exists in intracellular micro-environment only when the cell membrane is intact, while it could be released into cell culture medium when the cell membrane becomes disruptive. Therefore, LDH release assay has been used to evaluate cell membrane integrity [40]. The levels of LDH release from each treatment were calculated and presented in Fig. 9. Compared to the negative control (7.87% ± 0.75%, treated with naked pDNA), the LDH release levels from CAR-CBA-pDNA (40.12% ± 3.22%) and CHL-CBA-pDNA (18.41% ± 0.83%) were higher, but they were lower than that of the positive control (98.50% ± 0.63%, treated with LDH release reagent).

3.6. *Morphology of cell membrane after transfection*

DiI was used to stain cell membrane to show the image of cell membrane in red color, and the red image of cell membrane could reflect the integrity of cell membrane to some degree. As shown in Fig. 10, the red color of cell membrane's image for the negative control (exposed to naked pDNA) was uniform, while after cells were treated with 1% Triton X-100, the red color of cell membrane almost could barely be observed. For the groups of CAR-CBA-pDNA and CHL-CBA-pDNA, the images of cell membrane could be observed, even though the red color was weaker compared to the negative control, but more evident than the treatment group of 1% Triton X-100. To some content, the two cationic polymers destabilize the membrane favoring their entry into cells, but the skeleton of cell membrane transfected by the two polymers still remains.

4. Conclusion

The results of this research indicated that the introduction of guanidino groups could endow polymers of CAR-CBA and CHL-CBA unique nucleolus localization abilities. MCF-7 cells arrested at M phase are in favor of the transfection efficiencies of the two polymers, and it is unadvisable to perform transfection on cells arretd at G2 phase. According to the results of endocytosis inhibitor treatments coupled with endosomal/lysosomal escape ability studies of complexes, we

could confirm that the internalization of CAR-CBA-pDNA is dependent on clathrin-mediated endocytosis, and CAR-CBA-pDNA could escape from endosomes/lysosomes. While the cellular uptake of CHL-CBA-pDNA maybe occur via clathrin- and caveolae-independent endocytosis. The differences of structural and physio-chemical property between CAR-CBA and CHL-CBA, such as the molecular weight, zeta potential, flexibility of structure, amount and position (main chain or side chain) of guanidine groups, could make their endocytosis mechanisms different.

Conflicts of interest statement

All authors declare that there are not any potential conflicts of interest.

Acknowledgments

This work was supported by National Natural Science Foundation of China (Grant no. 81373335). We appreciate the Department of Pharmacology Teaching and Research at China Medical University for their great assistance in providing experimental apparatus, MCF-7 cell line and *E. coli* containing plasmids of pcDNA3.1-EGFP.

REFERENCES

[1] Thomas CE, Ehrhardt A, Kay MA. Progress and problems with the use of viral vectors for gene therapy. Nat Rev Genet 2003;4(5):346–58.
[2] Baum C, Kustikova O, Modlich U, Li Z, Fehse B. Mutagenesis and oncogenesis by chromosomal insertion of gene transfer vectors. Hum Gene Ther 2006;17(3):253–63.
[3] Singer O, Verma IM. Applications of lentiviral vectors for shRNA delivery and transgenesis. Curr Gene Ther 2008;8(6):483–8.
[4] Pedroso de Lima MC, Simões S, Pires P, Faneca H, Düzgüneş N. Cationic lipid–DNA complexes in gene delivery: from biophysics to biological applications. Adv Drug Deliv Rev 2001;47(2–3):277–94.
[5] Ferruti P, Marchisio MA, Barbucci R. Synthesis, physico-chemical properties and biomedical applications of poly(amido amine)s. Polymer 1985;26(9):1336–48.
[6] Pack DW, Hoffman AS, Pun S, Stayton PS. Design and development of polymers for gene delivery. Nat Rev Drug Discov 2005;4(7):581–93.
[7] Ferruti P, Marchisio MA, Duncan R. Poly(amido-amine)s: biomedical applications. Macromol Rapid Commun 2002;23(5–6):332–55.
[8] Meng FH, Hennink WE, Zhong ZY. Reduction-sensitive polymers and bioconjugates for biomedical applications. Biomaterials 2009;30(12):2180–98.
[9] Sirri V, Urcuqui-Inchima S, Roussel P, Hernandezverdun D. Nucleolus: the fascinating nuclear body. Histochem Cell Biol 2008;129(1):13–31.
[10] Pyper JM, Clements JE, Zink MC. The nucleolus is the site of Borna disease virus RNA transcription and replication. J Virol 1998;72(9):7697–702.
[11] Brunner S, Fürtbauer E, Sauer T, Kursa M, Wagner E. Overcoming the nuclear barrier: cell cycle independent nonviral gene transfer with linear polyethylenimine or electroporation. Mol Ther 2002;5(1):80–6.
[12] Brunner S, Sauer T, Carotta S, Cotten M, Saltik M, Wagner E. Cell cycle dependence of gene transfer by lipoplex, polyplex and recombinant adenovirus. Gene Ther 2000;7(5):401–7.
[13] Frankel AD, Pabo CO. Cellular uptake of the tat protein from human immunodeficiency virus. Cell 1988;55(6):1189–93.
[14] Khalil IA, Kogure K, Akita H, Harashima H. Uptake pathways and subsequent intracellular trafficking in nonviral gene delivery. Pharmacol Rev 2006;58(1):32–45.
[15] Torchilin VP, Rammohan R, Weissig V, Levchenko TS. TAT peptide on the surface of liposomes affords their efficient intracellular delivery even at low temperature and in the presence of metabolic inhibitors. Proc Natl Acad Sci USA 2001;98(15):8786–91.
[16] Wender PA, Galliher WC, Goun EA, Jones LR, Pillow TH. The design of guanidinium-rich transporters and their internalization mechanisms. Adv Drug Deliv Rev 2008;60(5):452–72.
[17] Nimesh S, Chandra R. Guanidinium-grafted polyethylenimine: an efficient transfecting agent for mammalian cells. Eur J Pharm Biopharm 2008;68(3):647–55.
[18] Grecco HE, Schmick M, Bastiaens PIH. Signaling from the living plasma membrane. Cell 2011;144(6):897–909.
[19] Yan Y, Such GK, Johnston AP, Best JP, Caruso F. Engineering particles for therapeutic delivery: prospects and challenges. ACS Nano 2012;6(5):3663–9.
[20] Albanese A, Tang PS, Chan WCW. The effect of nanoparticle size, shape, and surface chemistry on biological systems. Annu Rev Biomed Eng 2012;14(1):1–16.
[21] Herd H, Daum N, Jones AT, Huwer H, Ghandehari H, Lehr CM. Nanoparticle geometry and surface orientation influence mode of cellular uptake. ACS Nano 2013;7(3):1961–73.
[22] Kumari S, Mg S, Mayor S. Endocytosis unplugged: multiple ways to enter the cell. Cell Res 2010;20(3):256–75.
[23] Nam HY, Kwon SM, Chung H, et al. Cellular uptake mechanism and intracellular fate of hydrophobically modified glycol chitosan nanoparticles. J Control Release 2009;135(3):259–67.
[24] Wang LH, Rothberg KG, Anderson RGW. Mis-assembly of clathrin lattices on endosomes reveals a regulatory switch for coated pit formation. J Cell Biol 1993;123(5):1107–17.
[25] Boussif O, Lezoualc'h F, Zanta MA, et al. A versatile vector for gene and oligonucleotide transfer into cells in culture and in vivo: polyethylenimine. Proc Natl Acad Sci USA 1995;92(16):7297–301.
[26] Conner SD, Schmid SL. Regulated portals of entry into the cell. Nature 2003;422(6927):37–44.
[27] Felgner PL, Gadek TR, Holm M, et al. Lipofection: a highly efficient, lipid-mediated DNA-transfection procedure. Proc Natl Acad Sci USA 1987;84(21):7413–17.
[28] Kim TI, Lee M, Kim SW. A guanidinylated bioreducible polymer with high nuclear localization ability for gene delivery systems. Biomaterials 2010;31(7):1798–804.
[29] Yu JK, Zhang JM, Xing HN, et al. Guanidinylated bioresponsive poly(amido amine)s designed for intranuclear gene delivery. Int J Nanomed 2016;11:4011–24.
[30] Xing HN, Lu M, Xian L, et al. Molecular weight determination of a newly synthesized guanidinylated disulfide-containing poly(amido amine) by gel permeation chromatography. Asian J Pharm Sci 2016;12(3):292–8.
[31] Tong JJ, Sun DD, Yang C, et al. Serum starvation and thymidine double blocking achieved efficient cell cycle synchronization and altered the expression of p27, p53, bcl-2 in canine breast cancer cells. Res Vet Sci 2016;105:10–14.
[32] Chang J, Jallouli Y, Kroubi M, et al. Characterization of endocytosis of transferrin-coated PLGA nanoparticles by the blood-brain barrier. Int J Pharm 2009;379(2):285–92.
[33] Swanson JA, Watts C. Macropinocytosis. Trends Cell Biol 1995;5(11):424–8.

[34] Vercauteren D, Vandenbroucke RE, Jones AT, et al. The use of inhibitors to study endocytic pathways of gene carriers: optimization and pitfalls. Mol Ther 2010;18(3):561–9.
[35] Zambrano F, Aguila L, Arias ME, Sánchez R, Felmer R. Improved preimplantation development of bovine ICSI embryos generated with spermatozoa pretreated with membrane-destabilizing agents lysolecithin and Triton X-100. Theriogenology 2016;86(6):1489–97.
[36] Gerlich D, Beaudouin J, Kalbfuss B, Daigle N, Eils R, Ellenberg J. Global chromosome positions are transmitted through mitosis in mammalian cells. Cell 2003;112(6):751–64.
[37] Michihara A, Toda K, Kubo T, Fujiwara Y, Akasaki K, Tsuji H. Disruptive effect of chloroquine on lysosomes in cultured rat hepatocytes. Biol Pharm Bull 2005;28(6):947–51.
[38] Wattiaux R, Laurent N, Wattiaux-De Coninck S, Jadot M. Endosomes, lysosomes: their implication in gene transfer. Adv Drug Deliv Rev 2000;41(2):201–8.
[39] Liu M, Li ZH, Xu FJ, et al. An oligopeptide ligand-mediated therapeutic gene nanocomplex for liver cancer-targeted therapy. Biomaterials 2012;33(7):2240–50.
[40] Dubois JLN, Lavignac N. Cationic poly(amidoamine) promotes cytosolic delivery of bovine RNase A in melanoma cells, while maintaining its cellular toxicity. J Mater Chem B 2015;3(31):6501–8.